BEAM MEASUREMENTS AT LCLS*

J. Frisch, R. Akre, F.-J. Decker, Y. Ding, D. Dowell, P. Emma, S. Gilevich, G. Hays, Ph. Hering, Z. Huang, R. Iverson, R. Johnson, C. Limborg-Deprey, H. Loos, E. Medvedko, A. Miahnahri, H.-D. Nuhn, D. Ratner, S. Smith, J. Turner, J. Welch, W. White, J. Wu, Stanford Linear Accelerator Center, Menlo Park CA 94025, U.S.A

Abstract

The LCLS accelerator is presently in a commissioning phase[1] and produces a 14GeV beam with normalized emittances on the order of one mm-mr, and peak current exceeding 3000 Amps. The design of the beam measurement system relies heavily on optical transition radiation profile monitors, in conjunction with transverse RF cavities, and conventional energy spectrometers. It has been found that the high peak currents and small longitudinal phase space of the beam generate strong coherent optical emission that limits the quantitative use of OTR and other prompt optical diagnostics, requiring the use of wire scanners or fluorescent screen based measurements. We present the results of beam measurements, measurements of the coherent optical effects, and future plans for the diagnostics.

LCLS ACCELERATOR

The Linac Coherent Light Source is a SASE Free Electron Laser, designed to produce X-rays with wavelengths down to 1.5 Angstroms, using electron beam energies up to 13.6 GeV.

Table 1: Accelerator Design Specifications

Energy	4.3 to 13.6 GeV
Bunch Charge	200 pC to 1 nC
Design emittance	~ 1.2 mm-mr slice
Peak current	~ 3.4 KA.
Repetition rate	120Hz, single pulse

An accelerator layout with beam parameters is given in figure 1.

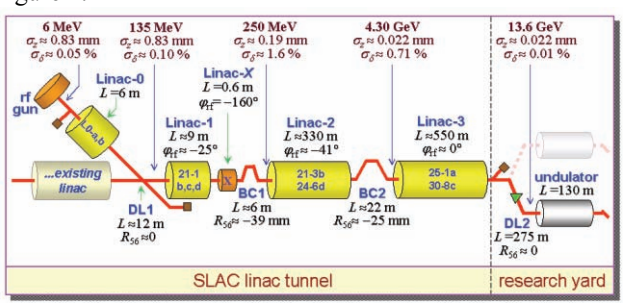

Figure 1: Accelerator layout.

Linac-2 and Linac-3 are only slightly modified from their configuration for the SLC [2]. The remainder of the machine is new, though it makes use of some old SLAC accelerator structures and magnets. As of April 2008, the beam is accelerated to the end of Linac-3 with nominal parameters, except that the repetition rate is presently limited to 30 Hz during commissioning.

BEAM DIAGNOSTICS AND MEASUREMENTS

The LCLS design relies heavily on beam-based control and feedback, necessitating the use of a variety of beam measurement devices:

- Position: Stripline BPMs
- Charge: BPMs, Toroids, Faraday Cups
- Beam Loss: Ion chambers and PMTs
- Profile: Wire Scanners, Optical Transition Radiation monitors, and fluorescent screens
- Emittance: Multiple profile monitors, or Quadrupole magnet gradient scans on a single profile monitor.
- Longitudinal Measurements: Spectrometers, Millimeter wave bunch length monitors, Transverse RF deflection cavities.

Beam Position Monitors

The LCLS injector, and a few locations along the Linac use self-calibrating strip-line BPMS based on digital down conversion: figure 2.

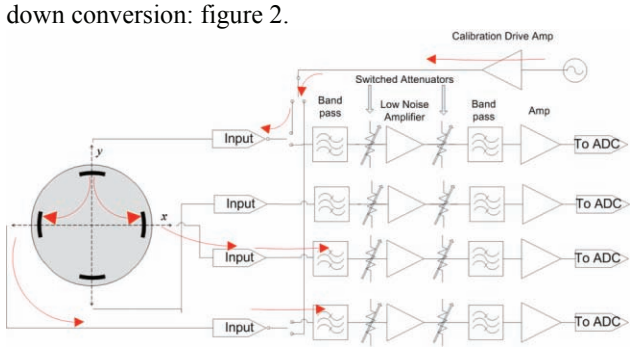

Figure 2: BPM Electronics

The BPMS operate at a center frequency of 140MHz, with a 7 MHz bandwidth. On every pulse, a tone burst is injected onto one strip, and the coupling to the perpendicular strips is measured. This corrects for gain changes in the readout channels and cables. [3]

The BPM noise is measured by performing a linear regression between the BPM under test, and the other BPMS in the accelerator, with the residual indicating the position noise, figure 3.

*Work supported by DOE Contract DE-AC02-76SF00515

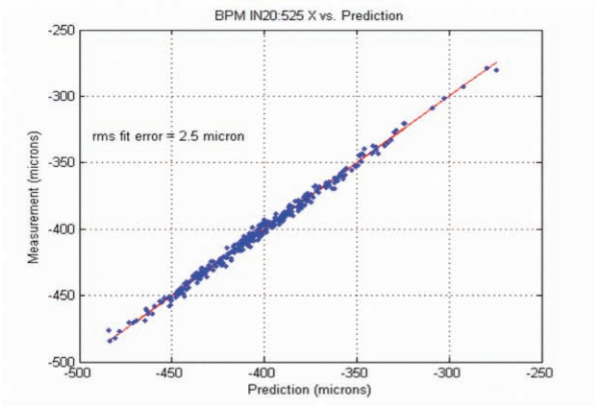

Figure 3, Example BPM noise measurement (at 350 pC) with 2.5 micron resolution demonstrated.

At 200pC, the BPMs meet the 5 micron RMS noise specification, with typical noise of 3 microns. Figure 4 shows the X and Y beam positions after BC1, measured over 24 hours. Note that the regular jumps are beam measurements. The beam motion is approximately 15 microns RMS at a location where the beam size is typically 50 microns RMS.

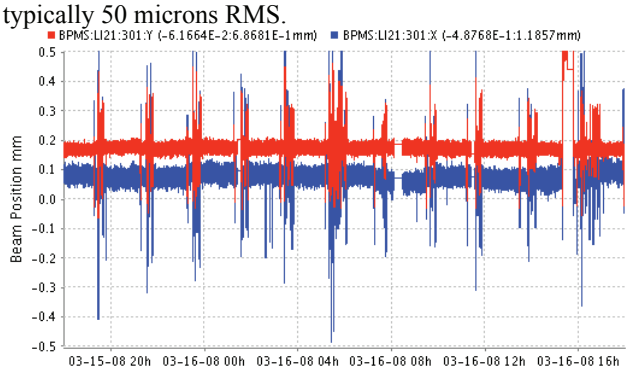

Figure 4, Beam position stability over 24 hours

Beam Charge Measurement

The LCLS BPMs provide a low noise ($7x10^{-4}$ RMS) relative beam charge measurement, but do not provide an absolute calibration. Absolute calibration is done using toroids in the LCLS injector, and existing (independently calibrated) toroids in the SLAC beam switchyard at 13.6 GeV. The two types of toroids agree within 5%.

The LCLS injector has 2 faraday cups at the 6MeV gun energy, with one in the straight-ahead line and one in the gun spectrometer. These faraday cups give a calibration that is 40% lower than observed with the toroids. These faraday "cups" are actually plates, and it is possible that a large amount of secondary electrons are lost, however the calibration error is not yet understood.

Beam Loss Measurement

The LCLS accelerator is designed to operate with minimal beam loss. The single pulse intensity is below the damage threshold for the accelerator; however average beam loss monitors are used to disable the beam to reduce the possibility of activation and electronics damage. Under normal conditions the beam loss is below the measurement limit of a few percent.

Beam Profile Measurement

The LCLS uses 3 different diagnostics for beam transverse profile measurement:

- Fluorescent Screens: These have good sensitivity, but saturate at high intensities (>~0.04pC/um^2) [4]. They are used in the LCLS injector at 135 MeV and lower energies.
- Wire Scanners: These have good resolution, and measurements are nearly non-invasive. However they only provide multi-pulse averaged, integrated profiles, and require long measurement times. Wire scanners are used in the LCLS energies of 135 MeV and above.
- Optical Transition Radiation Monitors: These have good resolution and linearity. OTR monitors are installed in the LCLS at 135MeV and higher energies, however, coherent optical effects prevent their quantitative use after the first bunch compressor.

Fluorescent Screens

The LCLS fluorescent screens use Ce:YAG crystals, 100 microns thick, oriented normal to the beam. 45 degree mirrors are located behind the crystals to reflect the light into cameras. This provides approximately 50 micron resolution.

The gun solenoid can be adjusted to image the cathode to the second YAG screen, located just before Linac-0. A mask placed at an image point in the drive laser beam, can produced a pattern on the cathode, and this will be imaged on the YAG screen. Figure 5 shows an electron beam image of a "LCLS" mask, at 6MeV. Imaging is performed at low currents ~30 pC.

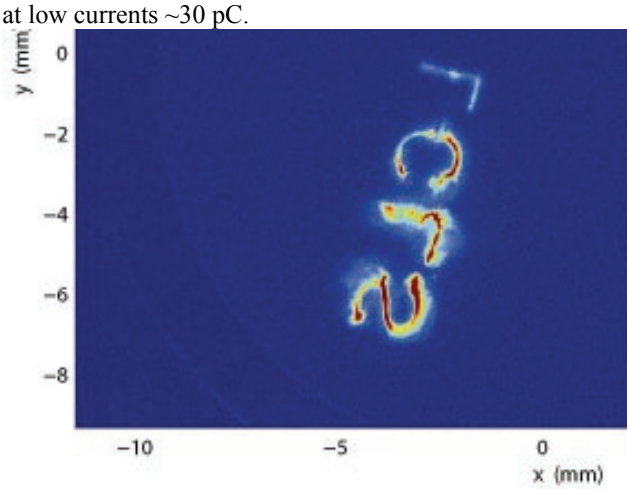

Figure 5, "LCLS" mask imaged onto YAG screen.

The imaging technique has proven useful for measuring the quantum efficiency of the cathode as a function of position. Typical quantum efficiencies are $5x10^{-5}$ at the nominal laser wavelength of 252nm. A cathode image is shown in figure 6 for 1.6mm diameter laser illumination.

Features in the emission pattern with a resolution of approximately 10 microns are observed.

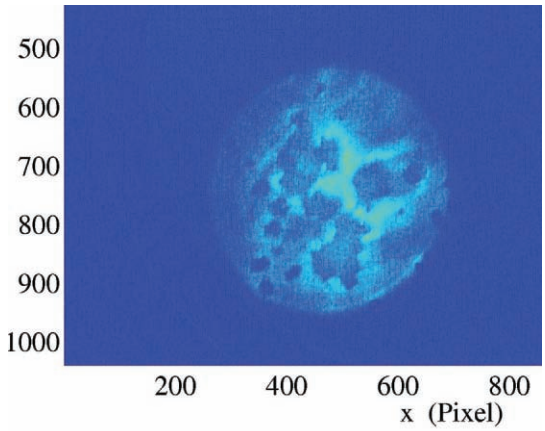

Figure 6. Electron beam cathode image with 1.6-mm spot diameter on the cathode

Wire Scanners

The LCLS wire scanners use 20-micron Tungsten wires driven by a stepper motor / leadscrew actuator. Scattered electrons are detected downstream by scintillators.

Initially the wire scanners used direct drive, with a step size of 5 microns. The wire vibration was found to be unacceptable and 10X gear reducers were added, reducing the vibration, but decreasing the maximum scan speed. With the reducers, the step size is now 0.5 microns. Figure 7,8 show a wire scan at 135MeV before and after the addition of the reduction gears.

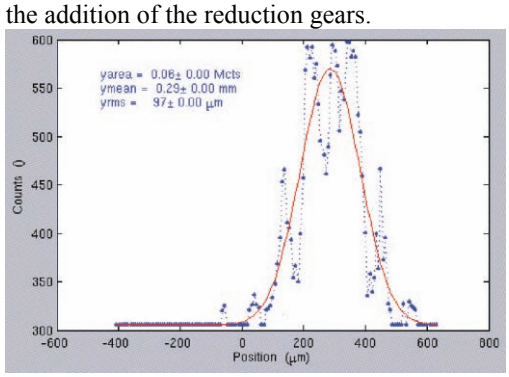

Figure 7. Wire scan at 135MeV

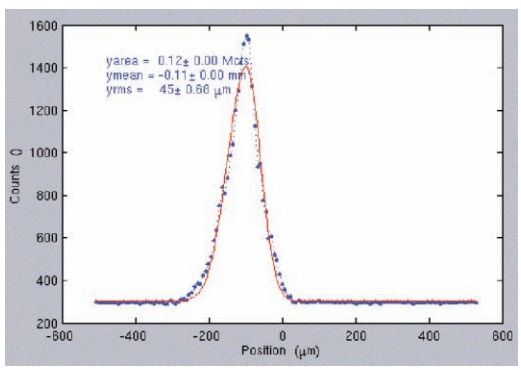

Figure 8. Wire scan at 135 MeV with 10X gear reducer added.

When wire scan or profile monitor data is used to provided a beam size, some fitting algorithm must be used to extract the RMS beam size. LCLS data analysis and emittance measurements use an asymmetric Gaussian fit, for the wire-scans, however results from other fit methods are recorded as well. Note that a choice of fit method can significantly change the measured beam size. Figure 9 shows an asymmetric Gaussian fitted to a beam with transverse tails (at 250 MeV, after the first bunch compressor).

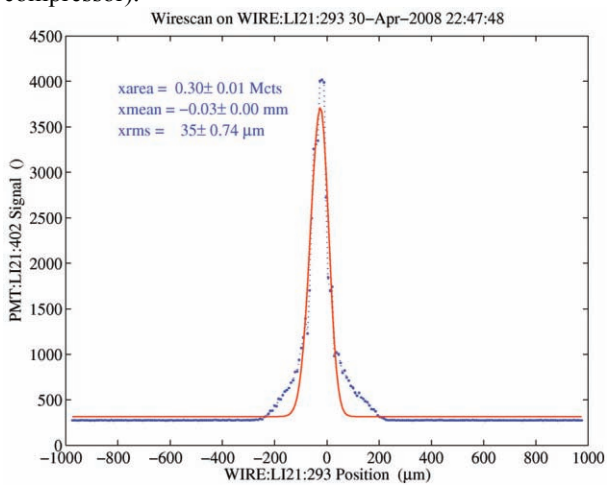

Figure 9. Wire-scan profile with fit (250MeV after BC1)

Optical Transition Radiation Monitors

At 135MeV and higher energies (after Linac-0), the beam size and charge in the LCLS are high enough to saturate fluorescent screens, and Optical Transition Radiation monitors with a 1-micron thick aluminum foil oriented at 45 degrees to the beam axis are used. The OTR camera is sensitive to wavelengths from 1 micron to 400 nanometers.

A beam image from an OTR at 135MeV is shown in figure 10. Note that the angle of the foil relative to the camera produces a position dependant focus, which limits the usable range to approximately +/-1 mm in the horizontal plane.

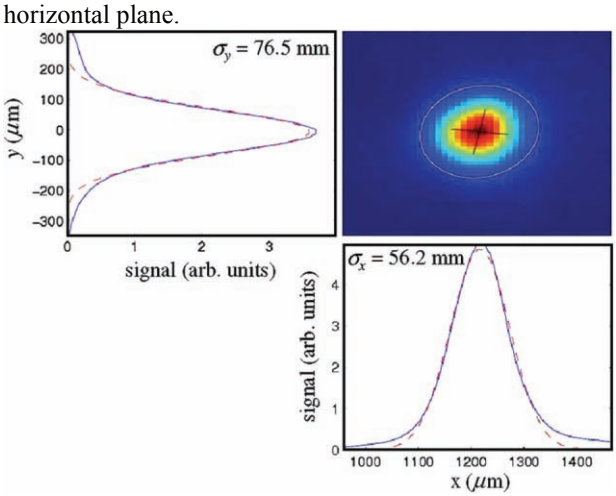

Figure 10. OTR Image at 135MeV

OTR profile monitors were intended as the primary transverse beam diagnostic in the LCLS. It has been discovered that the electron beam contains longitudinal structure at optical wavelengths, and that this distorts the OTR images.

Coherent Optical Transition Radiation

Optical transition radiation is emitted when an electron passes from vacuum into a conductor. For the extreme-relativistic beams used in accelerators, radiation is emitted broadband up to approximately the plasma frequency of the metal (~20eV). For details see [5]. In order for the radiated energy to be proportional to the electron charge, the emission from each electron in the beam must add incoherently.

If the beam has longitudinal structure on a scale comparable to the measurement wavelength, the beam can emit coherently, and the power will scale as the square of the charge. The LCLS beam contains on the order of 10^6 electrons in an optical wavelength, so even a density modulation of 10^{-3} will produce significant coherent emission.

Coherent OTR effects can be seen in the LCLS injector after DL1 (see Fig. 1), but before the beam is compressed. The field gradient of a dispersion correction quadrupole magnet in the DL1 bend is varied, and the image on an OTR screen at the end of L1 is recorded. For this experiment the RF in L2 is phased on the RF crest, and the bunch compressor BC1 is turned off (straight ahead beam, no dispersion). Figure 11 shows the integrated OTR intensity varying, and figure 12 shows the non-parabolic variation of measured Y beam size at the OTR. The measured beam size changes are not believed to represent actual changes in electron beam size, but rather changes in the distribution of the coherent optical signal. These changes (~25%) are large enough to invalidate emittance measurements. Note that the integrated optical signal is measured in uncalibrated "counts", the sum of the intensities of the pixels in the OTR image.

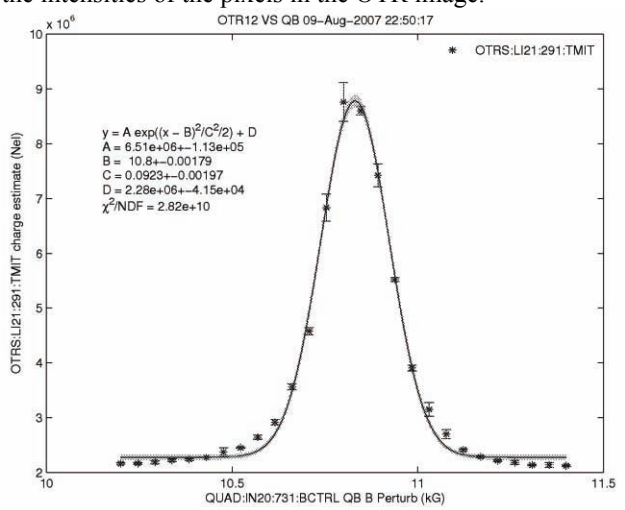

Figure 11. Integrated OTR intensity as the DL1 quadrupole magnetic field gradient is varied

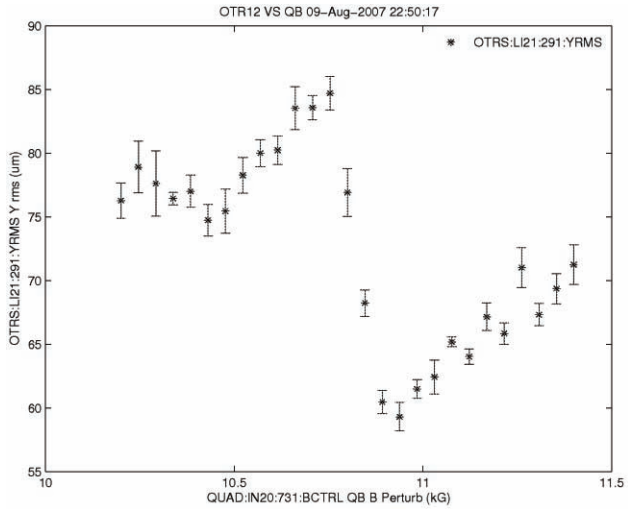

Figure 12. Measured Y beam size as the DL1 quadrupole magnetic field gradient is varied

The observed coherent OTR effects are larger after the first bunch compressor. This is presumably due to length compression of longitudinal structure on the beam, and longitudinal dispersion converting energy modulation into density modulation.

An OTR foil can be inserted in the first bunch compressor chicane. This has the effect of washing out any temporal structure on the beam, and also increasing the emittance at the end of the compressor. If we observe the OTR foil after the bunch compressor with the chicane foil inserted or removed, we see an approximate factor of 10 change in integrated optical signal level, Figures 13, 14.

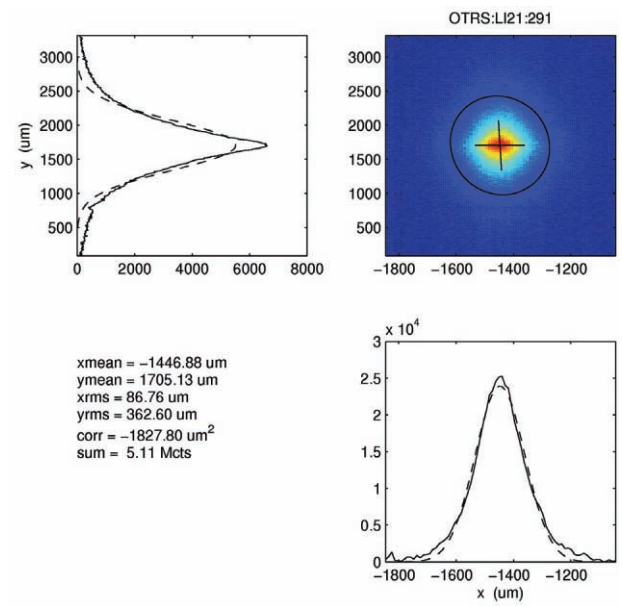

Figure 13, OTR with foil inserted in chicane. Integrated signal 5.11×10^6 counts.

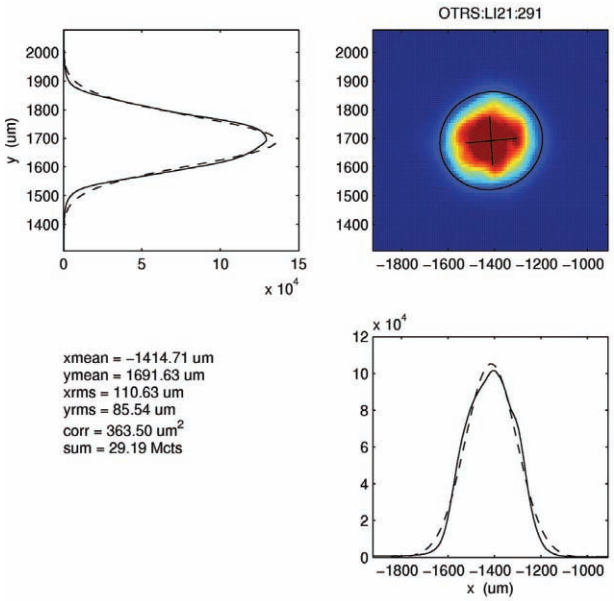

Figure 14, OTR with foil in chicane removed, integrated signal 2.9x107 counts . (6x107 counts without saturation)

If the phases of the structures in Linac-1 are adjusted to maximize compression in BC1, very dramatic COTR effects are observed. The toroidal shape is predicted from the circular polarization of the OTR emission. Interference produces an image that is proportional to spatial derivative of the original beam distribution [6]. Figure 15.

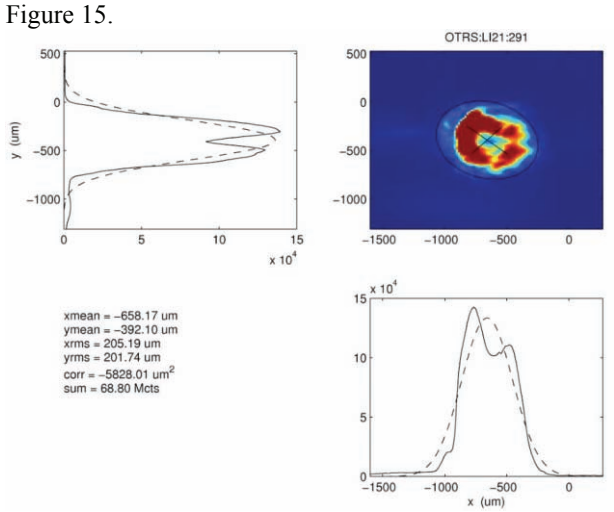

Figure 15. COTR with Linac-1 phases set for maximum compression in BC1. Integrated signal 100X incoherent.

In the second bunch compressor, the peak currents are higher, the coherent effects much stronger, producing distorted beam images, figure 16.

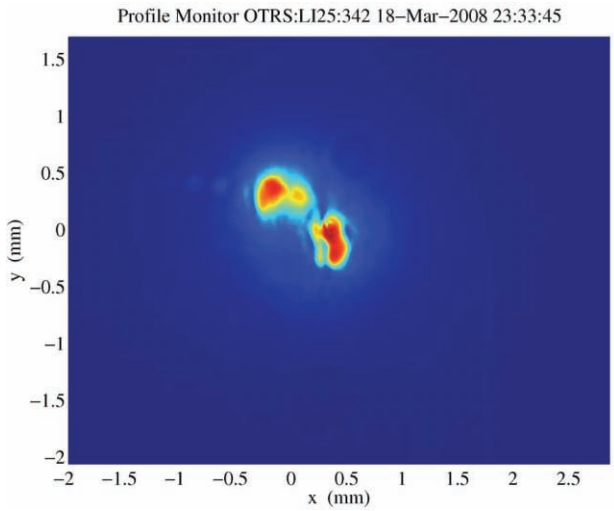

Figure 16. OTR image after second bunch compressor, normal compression, 1nC charge.

A diffraction grating was added to the OTR after the second bunch compressor to allow an approximate measurement of the spectrum of the coherent emission. The emission was found to be broadband over the camera's wavelength range of approximately 400nm to 1 micron (Figure17). This image is under normal compression conditions in BC1 and BC2. Note that the incoherent signal is too dim to observe in this image.

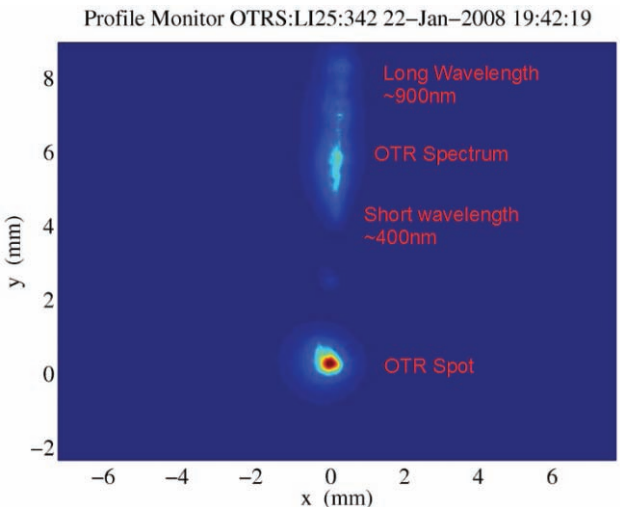

Figure 17. Spectrum of coherent OTR emission.

As expected, the strongest coherent OTR signal is seen when the bunch is maximally compressed in the second bunch compressor. The optical spectrum is seen to have spatial dependence, possibly due to a combination of coherent OTR effects and CSR beam breakup. Figure 18

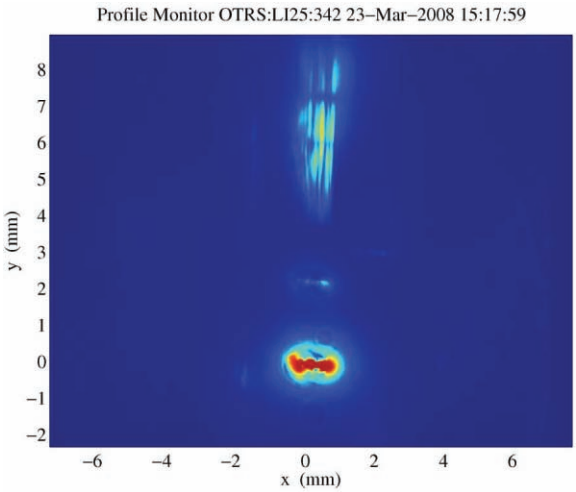

Figure 18. OTR image at maximum bunch compression in second bunch compressor.

Coherent Optical Transition Radiation Mitigation

The coherent optical effects make OTR profile monitors unusable for quantitative studies in the LCLS after DL1 (135MeV). The existing cameras are only sensitive to wavelengths longer than 400nm, and coherent effects are seen at this wavelength. We will investigate coherence at wavelengths as short as 200nm, roughly the limit of conventional optics, but the small longitudinal phase space of the beam may support modulations at even shorter wavelengths.

The LCLS plans to install a "laser heater" [7] before DL1 to increase the longitudinal phase space of the beam and reduce longitudinal space charge and CSR microbunching. This will likely also reduce or eliminate the coherent OTR effects. Until it is installed, however, the LCLS must rely on wire scanners for beam profile measurements.

The normal optics for the LCLS injector produces a ~50um beam waist after L0. Longitudinal space charge field at this waist may convert beam shot noise density fluctuation to energy modulation, at and near the optical wavelengths, which then produces amplified density modulation by DL1. Adjusting the optics to remove this waist may reduce the coherent OTR effects, but this has not yet been tested.

Emittance Measurements

The LCLS beam emittance is measured by one of two methods.

1. Scan a quadrupole magnet and measure the beam profile near the waist
2. Measure the beam profile at several locations with known phase advance.

Wire scanners are used for profile measurement throughout the machine, and an OTR screen can be used upstream of DL1 (at 135MeV).

The emittance measurement is completely automated by software that reads the machine model and drives wires scanners or OTR monitors for either quad-scan or multi-screen measurements. A quad-scan, wire scanner emittance measurement at 135 MeV, and 1nC is shown in figures 19 and 20.

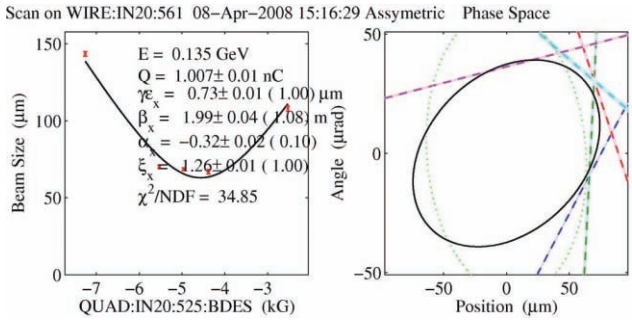

Figure 19, Horizontal emittance of 0.73um, at 1nC. And 135MeV, calculated using asymmetric Gaussian fits.

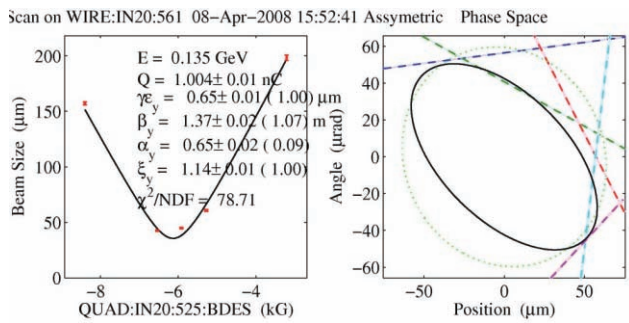

Figure 20, Vertical emittance of 0.65 um at 1nC and 135 MeV calculated using asymmetric Gaussian fits.

The measurements in figure 19 and 20 represent approximately the best measured emittance for the Gun / L0, at 1nC. More typical measurements are 0.8 to 1 micron. The emittance before the bunch compressor does not show a significant decrease at lower bunch charges, possibly due to the larger amount of time spent optimizing the system at 1nC.

The emittance is also measured after the first bunch compressor with a wire and quadrupole scan. Figures 21, 22 show an emittance x=1.15, y = 1.02 microns at 1nC. At 250pC, emittances of about 0.8 microns in both planes are commonly observed. Measurements were done at normal compression in BC1 (1 mm -> 200 microns). Horizontal emittances as 0.68 microns at 1nC have been measured. After BC1. The emittance measurements at the end of Linacx-3 show much more variable results ranging from 1 to 5 microns in both planes, with the best results observed with 250pC of bunch charge.

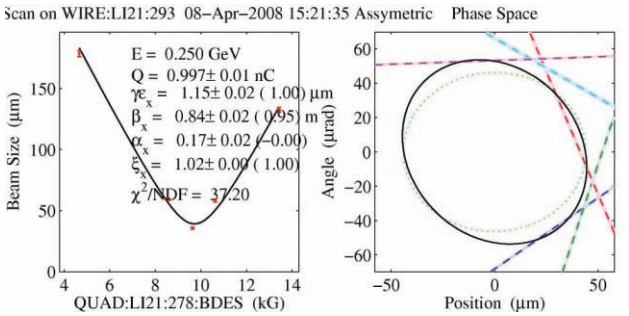

Figure 21. Horzontal emittance based on wire-scanner after first bunch compressor (1.15 microns)

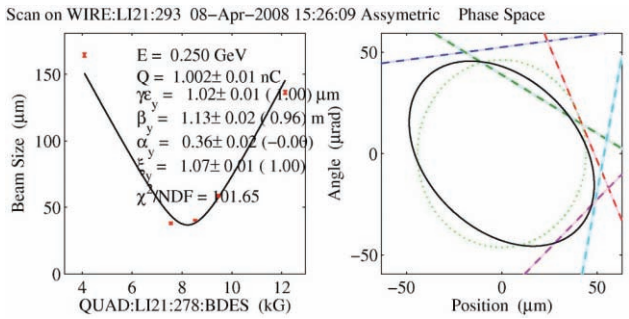

Figure 22.Vertical emittance based on wire scanner after first bunch compressor (1.02 microns).

Energy Spectrum Measurements

The beam energy spectrum can be measured at 5locations

- Gun spectrometer at 6 MeV, using a fluorescent screen.
- Injector Spectrometer, or DL1 bend at 135MeV (before compression), using an OTR screen.
- First bunch compressor at 250MeV, using an OTR screen.
- Second bunch compressor at 4.3 GeV using a OTR screen – however coherent effects make this a qualitative measurement only.
- Dump / spectrometer at the end of Linac-3 at 13.6 GeV, using a fluorescent screen.

The spectrometers are used to calibrate the energy gain of the gun and RF structures in the injector. They are frequently used with the transverse deflection cavities (next section) to provide energy vs. time measurements.

Bunch Temporal Measurements

An RF transverse deflection cavity, operating at a zero-crossing phase relative to the beam can be used to introduce a time-dependant transverse momentum. At a 90 degree betatron phase advance from the cavity, the temporal structure of the beam is transformed to transverse position. Transverse deflection cavities are located at 135MeV (before DL1 bend), and at 5 GeV (after the second bunch compressor) [8]. The transverse cavities deflect in the vertical direction to allow use in combination with the (horizontal) spectrometer magnets.

The coherent OTR effects prevent the use of the OTR screen originally intended for use with the transverse cavity after BC2 and instead a fluorescent screen at the end of L3 (13.6GeV) is used. Resolution, and the long fluorescence lifetime (~1 second) limit the accuracy of the measurement.

There is no transverse cavity directly after the first bunch compressor, however the second bunch compressor can be turned off, and L2 run at crest phase allowing the use of the transverse cavity located after BC2 to be used. Figure 23 shows the measured and *Elegant* simulated bunch length after the first bunch compressor (at 250 pC) as a function of the phase of the S-band system in Linac 1.

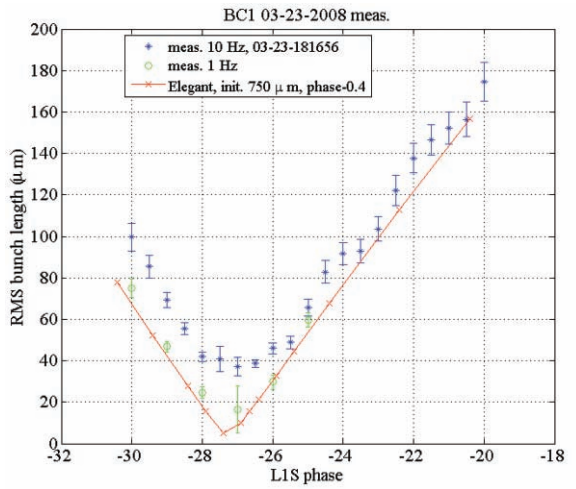

Figure 23. Bunch length after BC1 vs. pre-BC1 RF phase (see Fig 1) measured with BC2 off.

The perpendicular component of the RF phase in L2 can be adjusted to change the energy chirp and the compression in the second bunch compressor. Figure 24 shows the measured bunch length as the chirp is adjusted around the normal operating point, with a bunch charge of 250pC. A *Elegant* simulation, with an assumed input bunch length of 750 microns before BC1 is shown for comparison.

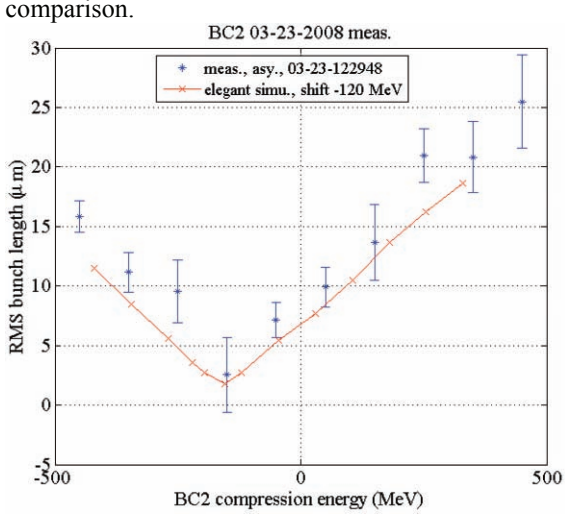

Figure 24. Bunch length after BC2 vs. RF chirp parameter. (250pC)

The minimum bunch length after BC2 is approximately 5 microns RMS. This represents the resolution of the transverse cavity system in conjunction with the fluorescent screen.

Energy vs. Time Measurements

The combination of transverse cavities and spectrometer magnets is a powerful tool for measuring the longitudinal beam phase space. Figure 25 shows the relative locations of the rf deflection cavity and the measurement locations.

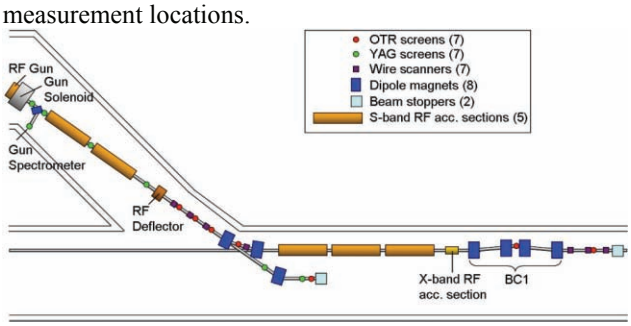

Figure 25. Transverse cavity location in injector

The injector RF deflector can be use in conjunction with either the injector spectrometer, or the DL1 bend to measure the longitudinal phase space of the beam after L0. (see figure 26).

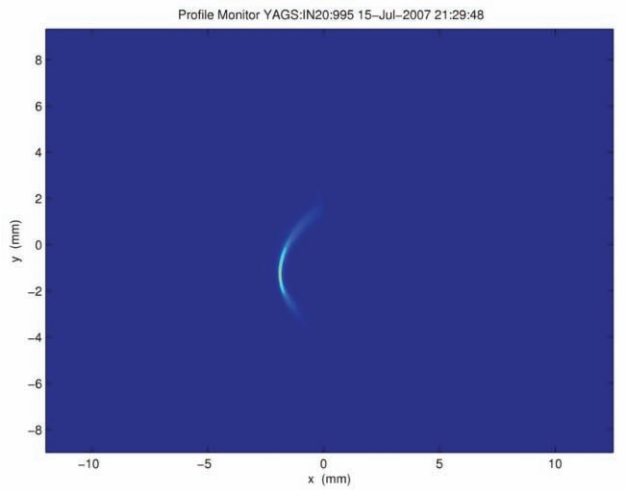

Figure 26. Energy vs. Time after L0 using the transverse RF deflector in the injector and spectrometer screen.

The first bunch compressor in the LCLS uses an 4th harmonic X-band RF (11.424 GHz) station to correct the phase space curvature (energy vs. time) which is introduced by the S-band RF structures. A plot of energy vs. time in the middle of BC1 allows adjustment of the X-band amplitude to linearize the energy chirp vs. time. Figure 27 shows energy vs. time in on the BC1 OTR screen without the X-band, figure 28 shows linear chirp with the X-band on. IN both cases the transverse RF deflector is switched on in order to provide a temporal measurement in the vertical direction.

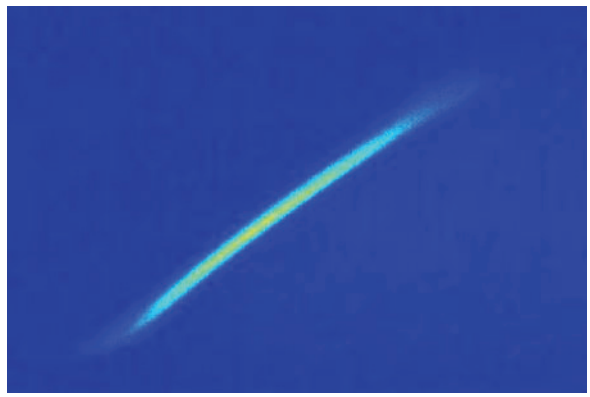

Figure 27. Energy vs. time in BC1, without X-band RF, (but with transverse RF deflector switched ON)

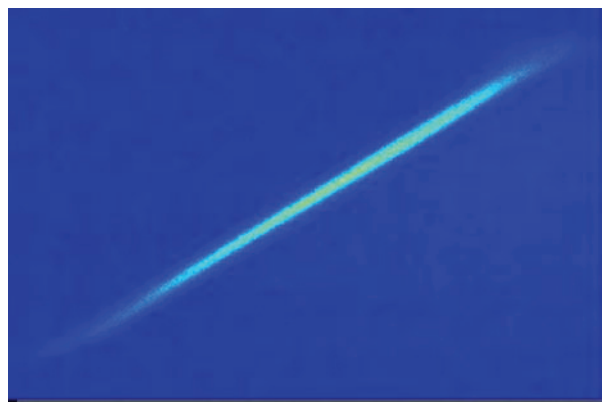

Figure 28. Energy vs. Time in BC1, with X-band RF (and with transverse RF deflector switched ON).

Relative Bunch Length Measurement

The transverse deflection cavities provide a high resolution and accurate bunch length measurement, but are invasive to beam operation. The RF phases in the LCLS drift over time and non-invasive bunch length monitors are required for feedback.

When an electron bunch passes through an impedance mismatch, it will emit electromagnetic radiation. For wavelengths long compared with the bunch length, the electrons in the bunch will radiate coherently. If we measure the radiated power at wavelengths comparable to the bunch length, the radiated power will vary with bunch length. This signal is not calibrated, but can be used to maintain a bunch length that has been set using the transverse cavities.

The bunch lengths after the first bunch compressor will produce radiation with wavelengths around 1 mm (300 GHz), while the beam after the second bunch compressor will be coherent at wavelengths below about 100 um, (3 THz).

Two relative bunch length monitors are installed after the first bunch compressor:

- Ceramic gap with waveguide coupled diodes at frequencies of 100 GHz and 300GHz.

- Diffraction / synchrotron / edge radiation monitor with an in-vacuum mirror and pyroelectric detectors.

The ceramic gap / RF diode monitor was simple to construct and provides a good bunch length signal (figure 29), however this technology does not work at the higher frequencies required for the second bunch compressor.

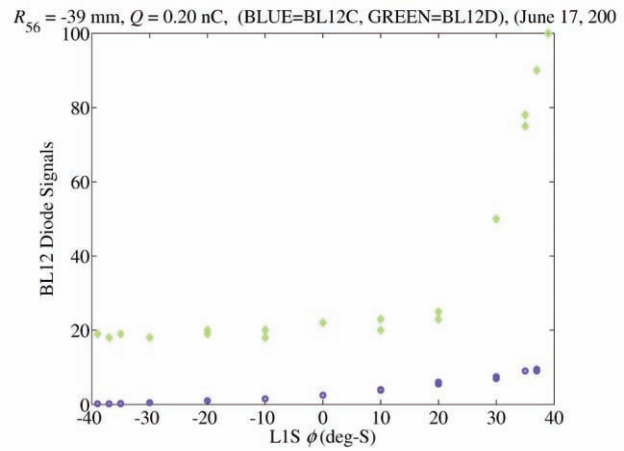

Figure 29. Ceramic gap / RF diode bunch length monitor, 100GHz and 300GHz diode signals as Linac 1 compression phase is varied.

The pyroelectric detector based bunch length monitor is located after the last bend magnet of the first bunch compressor. The signal is a combination of synchrotron radiation, end radiation, and diffraction radiation (figure 30). The bunch length monitor includes millimeter-wave filters to control the measurement frequency. For most operations however it was found that the unfiltered signal provided the lowest noise bunch length measurement. A scan of bunch length monitor signal vs. Linac 1 phase is shown in figure 31.

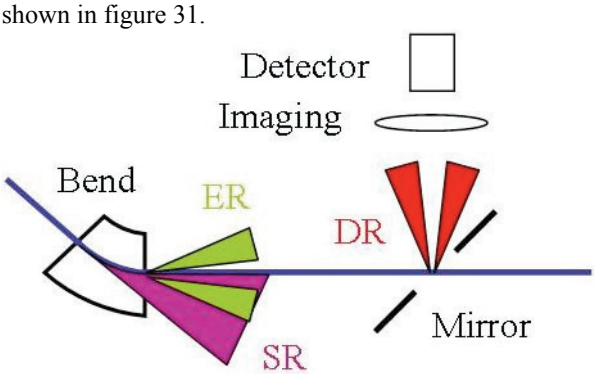

Figure 30. Pyroelectric bunch length monitor

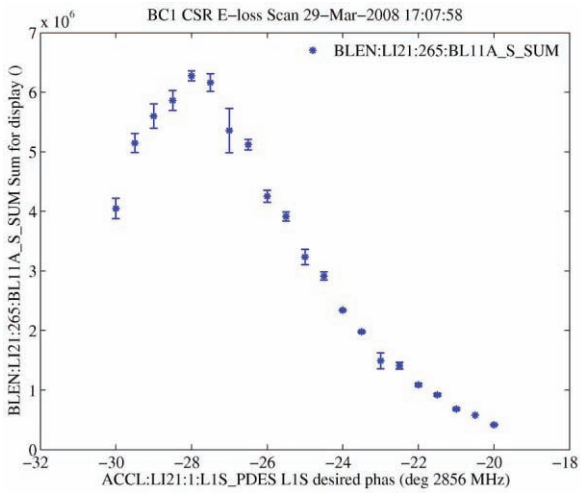

Figure 31. Signal from pyroelectric bunch length monitor as Linac 1 compression phase is varied.

The second bunch compressor uses a system very similar to the pyroelectric detector for BC1. A silicon vacuum window is used to provide transmission from 2 microns to millimeter wavelengths. Figure 32 shows the signal from this detector as the compression in BC2 is varied.

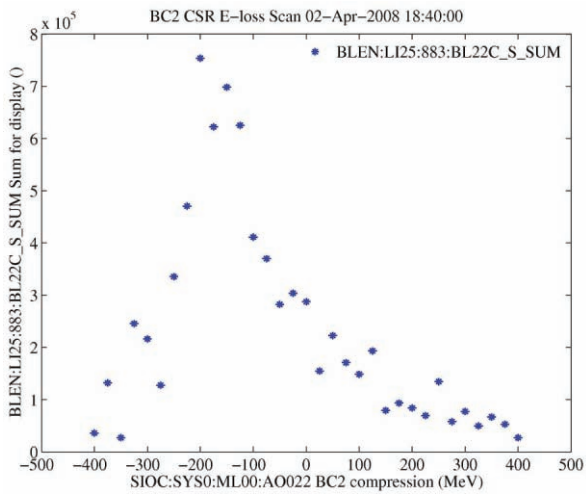

Figure 31. Signal from BC2 bunch length monitor as compression in L2 is varied.

Coherent Synchrotron Radiation

The coherent synchrotron radiation of a compressed bunch will produce increased energy spread, increased emittance and energy loss when the beam is close and over the full compression. The energy loss in the bunch compressor will result in the beam exiting the last compressor magnet with an x-angle. The X position (corresponding to energy loss) and emittance are shown and as the compression is change in BC1 are shown in figures 32 and 33.

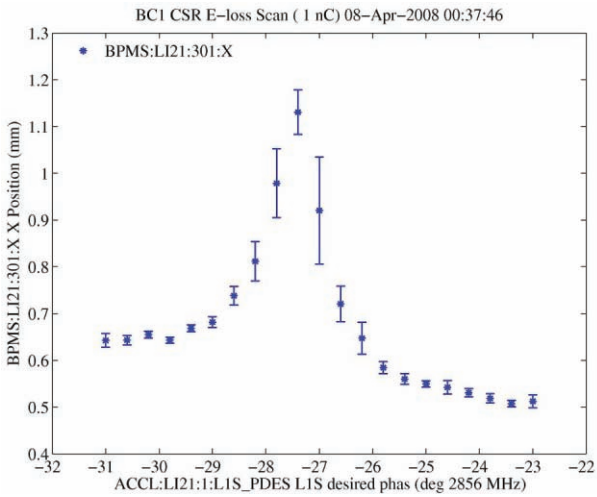

Figure 32. CSR energy loss in BC1 vs. RF phase

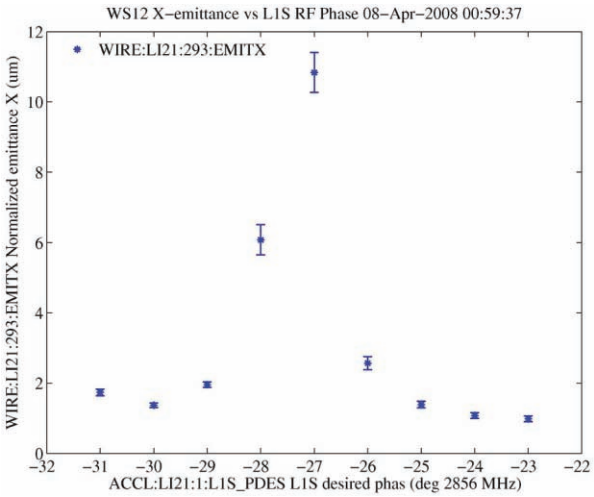

Figure 33. Horizontal emittance after BC1 due to CSR as compression (RF phase) is changed

A similar measurement of energy loss for the second bunch compressor is shown in figure 34.

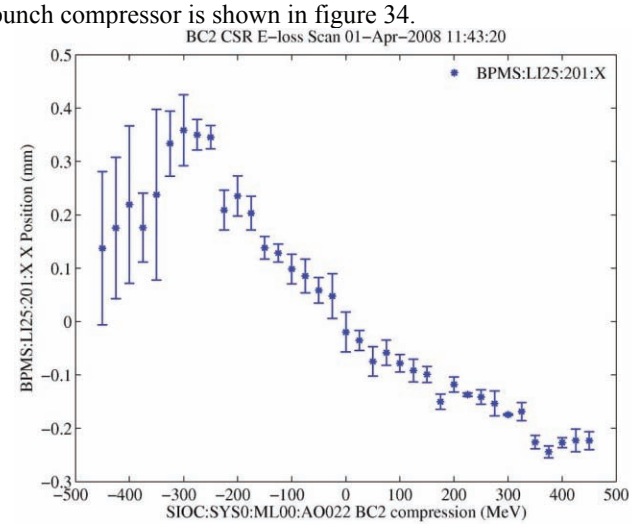

Figure34. Energy loss (as seen on BPM just downstream of BC1) due to CSR in second bunch compressor as compression is changed.

STATUS AND FUTURE WORK

The strong coherent optical transition radiation observed at LCLS has prevented the quantitative use of some diagnostics. In particular, there are no reliable beam profile measurements for the 900 meters of beamline between BC1 and the end of the L3 linac. A set of four wire-scanners were originally to be installed just upstream of BC2, but budget over-runs have forced a delay of these diagnostics. This lack of diagnostics has made beam tuning after the injector difficult.

There are several options to reduce the effects of COTR, including the addition of a “laser heater”, and optics changes in the injector, however the effectiveness of these is not yet known.

Despite the diagnostic limitations, the LCLS accelerator is operating at design charge, energy and bunch length. The emittance in the injector meets our requirements routinely, while the end of the linac is still quite variable. With additional tuning time, we expect to meet the emittance requirements at the end of the accelerator as well.

REFERENCES

[1] R. Akre et al, Phys. Rev. ST 11, 030703 (2008)
[2] R. Erickson, ed., “SLC Design Handbook”, Stanford (1984).
[3] E. Medvedko et al, “Stripline Beam Position Monitors for LCLS”, these proceedings.
[4] A. Murokh, “Limitations on Measuring a Transverse Profile of Ultra-Dense Electron Beams with Scintillator”, Proceedings 2001 Particle Accelerator Conference, Chicago.
[5] J. D. Jackson, “Classical Electrodynamics”, 1975, p685 .
[6] H. Loos, private communication
[7] Z. Huang et al. Phys Rev ST Accel Beams 8, 074401 (2004).
R. Carr, et.al. “Inverse Free Electron Laser Heater for the LCLS”, SLAC-PUB-11186, 2004.
[8] P. Emma et.al. “A Transverse RF Deflecting Structure for Bunch Length and Phase Space Diagnostics”, SLAC-PUB-8864, 2001